BJUI
BJU International

Original Article

Toward improved endoscopic examination of urinary stones: a concordance study between endoscopic digital pictures vs microscopy

Vincent Estrade[1] (iD), Baudouin Denis de Senneville[2], Paul Meria[3], Christophe Almeras[4], Franck Bladou[1], Jean-Christophe Bernhard[1], Gregoire Robert[1], Olivier Traxer[5] and Michel Daudon[6]

[1]Department of Urology, CHU Pellegrin, Bordeaux, [2]IMB, UMR CNRS 5251, University of Bordeaux, Talence Cedex, [3]Department of Urology, Saint-Louis Hospital, Denis Diderot University, Paris, [4]Department of Urology, La Croix du Sud Clinic, Quint Fonsegrives, [5]Department of Urology, Tenon Hospital, Pierre and Marie Curie University, Paris, and [6]Unit of Functional Explorations, Tenon Hospital, Pierre and Marie Curie University, Paris, France

Objective

To improve endoscopic recognition of the most frequently encountered urinary stone morphologies for a better aetiological approach in lithiasis by urologists.

Materials and Methods

An expert urologist intraoperatively and prospectively (between June 2015 and June 2018) examined the surface, the section, and the nucleus of all encountered kidney stones. Fragmented stones were subsequently analysed by a biologist based on both microscopic morphological (i.e. binocular magnifying glass) and infrared (i.e. Fourier transform-infrared spectroscopy) examinations (microscopists were blinded to the endoscopic data). Morphological criteria were collected and classified for the endoscopic and microscopic studies. The Wilcoxon–Mann–Whitney test was used to detect differences between the endoscopic and microscopic diagnoses. A diagnosis for a given urinary stone was considered 'confirmed' for a non-statistically significant difference.

Results

A total of 399 urinary stones were included in this study: 51.4% of the stones had only one morphological type, while 48.6% were mixed stones (41% had at least two morphologies and 7.6% had three morphologies). The overall matching rate was 81.6%. Diagnostics were confirmed for the following morphologies: whewellite (Ia or Ib), weddellite (IIa or IIb), uric acid (IIIa or IIIb), carbapatite-struvite association (IVb), and brushite (IVd).

Conclusions

Our preliminary study demonstrates the feasibility of using endoscopic morphology for the most frequently encountered urinary stones and didactic boards of confirmed endoscopic images are provided. The present study constitutes the first step toward endoscopic stone recognition, which is essential in lithiasis. We provide didactic boards of confirmed endoscopic images that pave the way for automatic computer-aided *in situ* recognition.

Keywords

aetiological lithiasis, morpho-constitutional analysis of urinary stones, flexible ureteroscopy training, endoscopic diagnosis, Laser fragmentation of stones, #EndoUrology, #KidneyStones, #UroStone

Introduction

A morpho-constitutional examination of urinary stones plays an essential role in the aetiological diagnosis [1–5]. The international morpho-constitutional classification of urinary stones includes six groups denoted by roman numerals (i.e. 'I' to 'VI'; Table 1). Each group is associated with a specific crystalline type: I, whewellite; II, weddellite; III, uric acid and urates; IV, calcium and non-calcium phosphates; V, cystine; and VI, other stones. Each type group is then divided into several subtypes to differentiate morphologies and aetiologies for a given crystalline type. Five morphological subtypes are encountered in whewellite Type I (differentiated by a lower case letter: Ia–Ie), each one being associated with a specific

Table 1 Morpho-constitutional classification of urinary stones.

Type	Surface	Section
Ia	Smooth or mammillary, dark-brown surface. Frequent papillary umbilication with a piece of Randall's plaque	Section showing compact concentric layers with a radiating organisation starting from a nucleus (often Randall's plaque)
Ib	Mammillary, rough surface. Colour: brown to dark brown	Unorganised section. Absence of umbilication
Id	Very smooth surface, beige or pale brown	Compact section showing thin concentric layers without radiations
Ic	Pale brown-yellowish budding surface (without any umbilication)	Loose, unorganised section. Light colour
Ie	Locally budding, mamillary or rough surface. Heterogeneous colour from brown-yellow pale to dark brown	Heterogeneous structure, with a mixture of poorly organised brown-yellow pale areas and locally concentric dark brown layers of radiating organisation
IIa	Yellow or light brown prickly, spiculated surface due to presence of aggregated bipyramidal crystals with sharp angles and edges	Loose radial crystallisation. Colour: pale brown-yellow
IIb	Yellowish or light brown surface with smooth, long bipyramidal crystals, resembling small desert roses	Compact poorly organised crystalline section. Colour: pale brown-yellow
IIc	Rough grey-beige to pale brown surface	Diffuse concentric structure at the periphery
IIIa	Homogeneous smooth surface. Colour: typically orange	Concentric layers with a radiating organisation around a well-defined nucleus. Colour: ochre to orange
IIIb	Rough and porous surface with a heterogeneous, beige to orange-red colour	Poorly organised, porous structure. Colour: ochre to orange
IIIc	Rough and locally porous beige or greyish surface	Unorganised porous section of the same colour as the surface
IIId	Heterogeneous, embossed, rough and porous surface with a greyish to dark brown colour	Alternating thick, brown and thin, beige layers with small porous zones
IVa1	Whitish, rough homogenous surface	Poorly organised structure, with loose concentric layers of the same colour as the surface
IVa2	Very peculiar morphology characterised by a yellow-brown, smooth surface with a glazed appearance and small cracks	Section showing irregularly arranged thin whitish and thick yellow-brown concentric layers
IVb	Heterogeneous surface, both embossed and rough. Heterogeneous colour from whitish to dark brown	Alternate thick whitish and thin brown-yellow layers
IVc	Aggregates of large crystals with blunt angles and edges. Colour: whitish	Diffuse, loose radial crystallisation. Whitish colour
IVd	Large rod-shaped crystals thereafter evolving toward slightly rough surface or resembling cabbage. Colour: whitish or beige	Radial crystallisation with locally concentric layers. Colour: whitish to beige
Va	Homogeneous, bumpy or rough, surface. Waxy aspect. Colour: light brown yellow	Diffuse radial organisation or unorganised section. Colour: light brown-yellow
Vb	Homogeneous smooth or finely rough surface, Colour: whitish to pale beige	Heterogeneous structure made of finely concentric microcrystalline beige organisation in the periphery around a compact, crystalline unorganised light brown-yellow core
VIa	Soft matrices, light brown in colour in contrast to other types of protein-rich calculi	Unorganised structure. Colour: light brown

aetiology. Practically: Ia = excessive concentration of oxalate in the urine induced by diet or default of diuresis, Ic = inherited primary hyperoxaluria, Ie = enteric hyperoxaluria induced by inflammatory bowel disease or by-pass. Interestingly, the most recent lithogenic events (in chronological order) are located on the surface of the stone, whereas less recent events are observable on a section of the stone. The nucleus of the stone, which is the oldest part, corresponds to the initial lithogenic context. Urinary stones are mixed (i.e. include at least two morphologies) in almost half of cases [5].

Daudon and Cloutier emphasised the importance of studying urinary stone morphologies [1,3,5] for an aetiological diagnosis of stone disease. A complete examination of the entire stone includes a visual morphological examination of the stone surface, the stone section, and the nucleus, as well as a spectrophotometric infrared recognition (Fourier transform-infrared spectroscopy [FTIR]) analysis of crushed stone fragments. However, it is now well established that modern endoscopic treatment of urinary stones relies on laser fragmentation [6–13]. Fragmentation, whether achieved with 'popcorn' [6] or 'dusting' modes [7], destroys the morphology of the targeted stone [8]. The morphological examination,

which is the first essential diagnostic step, is impossible to redo once the stone is destroyed. Moreover, Keller *et al.* [8] recently showed the impact of laser-based dusting on changes in stone composition with significant changes in the infrared spectra (particularly for weddellite, carbapatite, struvite, and brushite). Consequently, a FTIR examination of the stone powder itself does not provide sufficient information to determine correctly the lithogenic stage [1–5]. This finding reinforces the need to observe the morphology of the stone before laser-induced destruction to preserve an aetiological approach.

The present study constitutes the first step toward endoscopic stone recognition (ESR). We aimed to improve the recognition of the most frequently encountered urinary stone morphologies. Thus, an endoscopic-based examination of unfragmented stones was compared with microscopic observations of laser-fragmented stones, and a concordance study was conducted.

Materials and Methods

The study adhered to all local regulations and data protection agency recommendations (the National Commission on

Informatics and Liberty [CNIL]) dictates). Patients have been informed of the anonymous use of their data.
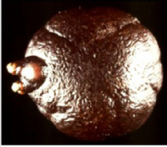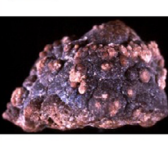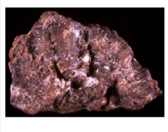
Endoscopic Study

An expert urologist (V.E., 20 years of experience) intraoperatively and prospectively examined stones between June 2015 and June 2018 using a flexible digital ureterorenoscope (Olympus URF-V charge-coupled device sensor; Olympus Corp., Tokyo, Japan). Visual cues that the surgeon has to consider for the estimation of a stone type are summarised in Table 1. The examination included a visual observation of the stone surface first, before laser fragmentation, then visual observation of the section and the nucleus and after laser stone section. Laser-based stone section in two parts was performed using the following laser parameters: frequency, 5 Hz; energy, 1.2–1.4 J; power, 6–7 W;

pulse length, short; fibre diameter, 230 or 270 μm [14,15]. That way, it was possible to fragment all types of pure and mixed stones. Once fragmented, the fragments were removed with a nitinol basket (Boston Zero Tip™ 1.9 F; Boston Scientific, Marlborough, MA, USA) through the ureteric access sheath (Coloplast ReTrace® 12/14 or 10/12 F; Coloplast, Humlebaek, Denmark). An additional fragmentation session was carried out when needed. Macro-fragments including at least one representative copy of the stone surface, the stone section and the nucleus were removed using a nitinol basket for subsequent examination in a dedicated laboratory.

Microscopic Study

The fragmented stones were subsequently analysed by a biologist (M.D., 40 years of experience) based on both

Fig. 1 Pure stone Type Ia or Ib.

	Pure Stone Type Ia or Ib: Component: whewellite Answers = 205: good match = 85% P = NS	
Descriptive anatomy of stone morphology	Microscopic reference images	Endoscopic images
Surface: *Ia:* Mamillary dark-brown surface. Frequent umbilication and Randall's plaque indicative of papillary origin *Ib:* brown to dark-brown, mamillary, rough surface	Ia Ib	Ia Ib
Section: *Ia:* made of compact concentric layers with radiating organisation starting from a nucleus. Colour: dark brown *Ib:* unorganised section and they never exhibit an umbilication	Ia Ib	Ia Ib
Common aetiology:	*Dietary hyperoxaluria, low diuresis (high oxalate concentration), Randall's plaque*	

morphological (i.e. binocular magnifying glass) and infrared (i.e. FTIR) analyses. Similar to the above-mentioned endoscopic analysis, the examination included the surface, the section and the nucleus of each stone.

Observations

The urinary stones were classified according to microscopic morphological instructions given by Daudon *et al.* [1]. We collected the following eight observations for all urinary stones in the endoscopic and microscopic studies.

- Three observations about surface morphology referred to as 'majority' (for the most visible morphology on the surface of the stone), 'secondary' (for potentially secondary visible morphology) and 'minority' (for another potentially visible morphology).
- Three observations about the inner structure: 'central' (for the morphology visible in the centre of the stone), 'peripheral' (for the morphology visible on the periphery of the stone) and 'intermediate' (for the morphology in between).
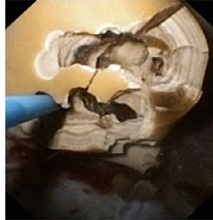
- Two observations about the nucleus: 'majority' (for the most visible morphology in the nucleus of the stone) and 'minority' (for another potentially visible morphology).

Concordance Between the Endoscopic- and Microscopic-based Observations

All data were collected into a single Excel spreadsheet that was retrospectively analysed using Matlab software (MathWorks, Inc., Natick, MA, USA).

We selected a subset of urinary stones for which 'Ia' or 'Ib' morphologies were encountered in any microscopic-based observation. Among these, urinary stones for which the 'Ia' or 'Ib' morphologies were encountered in any (resp. in none) endoscopic-based observation were listed and referred to as a 'good match'. The total number of urinary stones with a 'good match' was calculated and recorded. The Wilcoxon–Mann–Whitney test was used to determine whether the differences between endoscopic and microscopic diagnoses were significant. A significance threshold of $P = 0.05$ was used. A diagnosis for a given urinary stone was considered 'confirmed' for a non-significant difference between the

Fig. 2 Pure stone Type Id.

Figure N°2: Pure stone Type Id		
	Pure Stone Type Id: Component whewellite answers = 13: good match 92% *P* = NS	
Descriptive anatomy of stone morphology	Microscopic reference images	Endoscopic images
Surface: Very smooth surface, beige or pale brown in colour		
Section: Showing compact thin concentric layers without radiations. Colour: beige or pale brown		
Common aetiology:	*Malformative uropathy, stasis and confined multiple stones*	

endoscopic and microscopic examinations ($P > 0.05$). In such a case, the area under the receiver operating characteristic (ROC) curve (AUROC), sensitivity, specificity, positive predictive value (PPV) and negative PV (NPV) were calculated (considering the presence of a given morphology in the microscopic study as a 'positive case').

Results

Demographic Characteristics

In total, 399 urinary stones were included in this retrospective study. Among them, 48.6% were mixed stones (41% had at least two morphologies and 7.6% had three morphologies). Our cohort was composed of 63% calcium oxalate stones (Type I whewellite + Type II weddellite), 20% phosphate stones (Type IV carbapatite, brushite, and struvite), 15% uric acid and urate stones (Type III), 0.2% cystine (Type V), and 1.8% of other stones (Type VI).

Typical images obtained for each of the six urinary stone type groups are shown in Figs 1–9 respectively. Endoscopic- and microscopic-based observations of the stone surface and sections are reported, together with corresponding aetiological conditions.

Stone Morphologies Analysed

We identified 16 morphologies distributed over the following type groups:

- For whewellite Type I: Ia, Ib, Id and Ie
- For weddellite Type II: IIa and IIb
- For the uric acid and urate Type III: IIIa and IIIb
- For the calcium and non-calcium phosphate Type IV: IVa1 and IVa2 (carbapatite), IVb (carbapatite and struvite), IVc (struvite), IVd (brushite)
- For the cystine Type V: Va
- For the Type VI aggregating other stones (protein matrices ± whewellite): VIa and VIb

For this study, we grouped the following morphologies that had similar aetiologies: Ia and Ib, IIa and IIb, IIIa and IIIb, Va and Vb, and VIa and VIb.
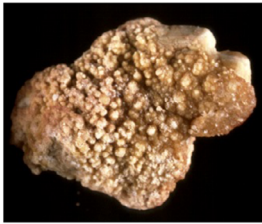
Fig. 3 Pure stone Type Ie.
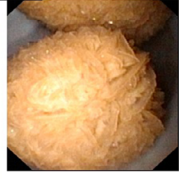
Figure N°3: Pure stone Type Ie		
	Pure Stone Type Ie : Component <u>whewellite</u> answers = 5: good match 80% P = NS	
Descriptive anatomy of stone morphology	Microscopic reference images	Endoscopic images
Surface: exhibit a locally budding, mamillary or rough brown-yellow pale surface		
Section: heterogeneous structure, with a mixture of poorly organised brown-yellow pale areas and of locally concentric dark brown layers with radiating organisation		
Common aetiology:	*Enteric hyperoxaluria, inflammatory bowel diseases (Crohn's disease), ileal resections, chronic pancreatitis.*	

Fig. 4 Pure stone Type IIa or IIb.

Figure N°4: Pure stone Type IIa or IIb		
	Pure Stone Type IIa or IIb: Component <u>weddellite</u> answers = 178: good match = 85% *P* = NS	
Descriptive anatomy of stone morphology	Microscopic reference images	Endoscopic images
Surface: *IIa*: Yellowish or light-brown prickly, spiculated surface due to the presence of aggregated bipyramidal crystals with sharp angles and edges *IIb*: yellow or light-brown surface with smooth, long bipyramidal crystals, thus resembling small desert roses	IIa IIb	IIa IIb
Section: *IIa*: loose radial crystallisation. Colour: yellowish to light brown *IIb*: compact poorly organised crystalline section	IIa IIb	IIa IIb
Common aetiology:	IIa: Hypercalciuria, whatever its origin, high molar ratio calcium/citrate IIb: Hypercalciuria ± hyperoxaluria ± hypocitraturia, Stasis, low diuresis	

Concordance Between the Endoscopic- and Microscopic-based Observations

Table 2 summarises the concordance between our endoscopic- and microscopic-based observations.

Morphologies Validated by the Microscopic and Endoscopic Examinations
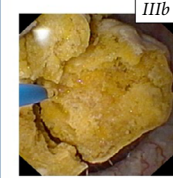
Diagnoses were confirmed for the following morphologies: whewellite (Ia or Ib: concordance = 85%, *n* = 205; Id: concordance = 92%, *n* = 12; Ie: concordance = 80%, *n* = 5), weddellite (IIa or IIb: concordance = 85%, *n* = 178), uric acid (IIIa or IIIb: concordance = 91% *n* = 64), carbapatite-struvite association (IVb: concordance = 50%, *n* = 10), brushite (IVd: concordance = 65%, *n* = 23). Several other pure stone morphologies depicted good matching, although just below the significance threshold of 0.05, such as carbapatite

(IVa1, concordance = 81%, *n* = 176). Other pure stone morphologies depicted excellent matching, but an insufficient number of cases, such as cystine (Va: concordance = 100%, *n* = 1).

Discussion

Our present study consisted of endoscopic recognition of the morphological elements constituting urinary stones before laser stone destruction. ESR allows the morphological identification of an entire stone and is thus essential in lithiasis. While the main objective of ESR is to identify a stone type, it also provides examinations of the anatomy of the excretory pathway, as well as the renal papillae. Flexible ureteroscopy is thus a great diagnostic and therapeutic candidate in lithiasis. We offer didactic boards to help with ESR comprised of reference images and descriptions (surface, section, and nucleus), and the lithogenic mechanisms and aetiologies associated with each morphology (Figs 1–6).
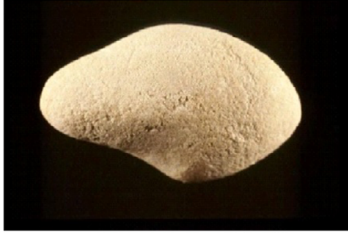
Fig. 5 Pure stone Type IIIa or IIIb.

Figure N°5: Pure stone Type IIIa or IIIb		
	Pure Stone Type IIIa and IIIb: Component uric acid <u>anhydrous</u> Answers = 64: good match = 91% P = NS	
Descriptive anatomy of stone morphology	Microscopic reference images	Endoscopic images
Surface: *IIIa:* Homogenous smooth surface. Colour: typically, orange *IIIb:* rough and porous surface with a heterogeneous, beige to orange colour and an orange-red	IIIa / IIIb	IIIa / IIIb
Section: *IIIa:* Compact concentric layers with a radiating organisation around a well-defined nucleus. Colour: ocher to orange *IIIb:* poorly organised, porous structure.	IIIa / IIIb	IIIa / IIIb
Common aetiology:	*IIIa: Low urine pH, stasis prostate hypertrophy, metabolic syndrome, ammoniagenesis defect* *IIIb: Insulin resistance, metabolic syndrome, type 2 diabetes, ammoniagenesis defect, low urine pH*	

It must be reported that a learning curve is needed to acquire the ESR skill, which may limit its translation to practical use. In the present study, the urologist (V.E.) had, first of all, to learn the classification of the different types of stone surface, section, and nuclei using the microscopic images provided by Daudon *et al.* [1,3,5]. Subsequently, he had to acquire the ability to recognise such types of stone surface, section, and nuclei on endoscopic images, based on the learned microscopic images and associated descriptions. Along this line, one goal of our concordance study is to reduce possible subjectivity in ESR and urologist bias by history. To make ESR easier for the urologist, we propose didactic boards of confirmed endoscopic images for the most frequently encountered urinary stones in daily practice. This follows the work of Bergot *et al.* [16], which showed that ESR teaching of junior urologists allows them to acquire the skill to recognise the most frequently encountered stones quickly. On the other hand, a computer-assisted approach delivers reproducible results and minimises operator dependency, as visual interpretation of stone images lacks a learning curve when the process is automated. It is therefore promising to train artificial intelligence algorithms with our confirmed endoscopic images. Black *et al.* [17] have recently shown that artificial intelligence (deep learning) applied to *in vitro* surface and section images of stones represents a great asset for the automatic recognition of whewellite, weddellite, uric acid, brushite, and struvite stones. Such algorithms may be able to do tests with various pre-defined score and error levels. Combined with our confirmed endoscopic images, deep neural networks, such as convolutional neural networks (CNN), which are able to process efficiently a high number of specific images and videos, are good candidates for automatic ESR.

In our present study, the FTIR examination detected 12 struvite cases that were not described using morphological analyses. The combination of morphological and FTIR examinations improved the diagnostic concordance of urolithiasis [1–4]. Our present findings of the epidemiological distribution of the different crystalline types, as well as the rate of pure/mixed stones are consistent with already published results [18]. Therefore, our present cohort is representative of the stone distribution that any urologist might encounter. Our study present confirmed the following

Fig. 6 Pure stone Type IVa1.

Figure N°6: Pure stone Type IVa1		
	Pure Stone Type IVa1: Component <u>carbapatite</u> Answers = 176 good match = 81% *P* = 0.03	
Descriptive anatomy of stone morphology	Microscopic reference images	Endoscopic images
Surface: whitish, rough homogeneous surface		
Section: poorly organised structure, with loose concentric layers of the same colour as the surface		
Common aetiology:	*Hypercalciuria, urinary tract infection.* *Aetiology may be oriented by the presence of other crystalline species and by the carbonatation rate of carbonated calcium phosphates*	

six morphological types: Ia or Ib, IIa or IIb, IIIa or IIIb, IVa, IVb and IVd. These six morphological types cover 95% of the most common pure stones that urologists encounter in their practice daily [5].

Our present study showed that recognising the main morphological surface criteria is easier than the other stages of the analysis (i.e. section and nucleus). This result is crucial because the majority of the surface area of a urinary stone represents recent lithogenesis. Its destruction by a laser *de facto* leads to a loss of aetiological information.

The enthusiasm of urologists for the laser spraying of calculations in the 'dusting' mode and the upcoming arrival of a new generation of very high frequency 'super thulium fibre' lasers [19,20] will positively affect the success of interventions to minimise the rate of residual fragments and improve results without fragments.

However, the urologist should not forget that the morpho-constitutional examination of a urinary stone, which is currently the only solution for observing the entire stone, is as important as the pathological examination of a surgical specimen for the therapeutic strategy of onco-urology cases.

Despite the variety of compositions and morphologies observed in urinary calculi, ~90% are composed of a limited number of crystalline species and morphological characteristics that are easily recognised through an endoscopic examination. The morpho-constitutional classification of urinary stones previously published is particularly suitable for this purpose. Endoscopic examination of 399 stones revealed good concordance between endoscopic and microscopic typing of the stones. For example, concordance of the results was observed in 86.1% of Type I

Fig. 7 Pure stone Type IVb.

Figure N°7: Pure stone Type IVb		
	Pure Stone Type IVb: Component <u>carbapatite</u> Answers = 10 good match = 50% *P* = NS	
Descriptive anatomy of stone morphology	Microscopic reference images	Endoscopic images
Surface: Heterogeneous surface, both embossed and rough, of clear to dark brown colour.		
Section: alternate thick whitish and thin brown-yellow layers		
Common aetiology:	*Urinary tract infection, Hypercalciuria, primary hyperparathyroidism*	

stones, 85% of Type II stones, 91% of Type III stones and 79% of Type IV stones made of calcium phosphate. Within stone types, it was possible to identify, with good agreement, specific subtypes related to a more accurate aetiological diagnosis, such as subtype Ia or Ib, which is mainly related to dietary hyperoxaluria due to oxalate-rich food intake or low diuresis, while subtype Ie is related to enteric hyperoxaluria. Subtype Id stones suggest stasis and anatomical confinement related to urological anomalies. The presence of a thin greyish layer on the surface of a subtype Ia stone is a marker for dietary hyperoxaluria in most cases. ESR may be more critical when mixtures of phosphates are present, as suggested by differences in concordance among the various subtypes. As shown in Table 2, concordance was high (~80%) for subtype IVa1 and IVb stones. In contrast, concordance was lower (65%) for subtype IVd, which is a marker for brushite-containing stones. Concordance was significantly better when brushite was the main component of the stone, reaching 77.8% of cases. However, the concordance between the endoscopic and microscopic examinations was only 21% for IVa2 stones, which are mainly composed of carbapatite. Two reasons could explain this low concordance. First, subtype

IVa2 is uncommon. Second, some morphological characteristics of these stones, such as the presence of tiny cracks within the structure, are reinforced by drying the stone before the microscopic examination, and thus could be less visible during the endoscopic analysis. Training based on an examination of a larger number of samples would improve the concordance for the stone types providing poor agreement between the endoscopic and microscopic examinations. Notably, the global concordance level was 81.6% in this first study.

As Almeras *et al.* [21] described a higher incidence of IVa2 stones when intrapapillary crystallisation occurred and others descriptions correlated to different lithogenesis mechanisms, the description of papillary abnormalities during flexible ureteroscopies would certainly add a diagnostic value to this ESR.

It should be emphasised that it is essential to record the traceability of the morphology of the surface, the section, and the nucleus of a urinary stone. The urologist must archive all images to allow retrospective expertise, if necessary, by a biologist, an expert urologist or machine learning.

Figure N°8: Pure stone Type IVd		
	Pure StoneType IVd: Component <u>brushite</u> N = 23: good match = 65% *P* = NS	
Descriptive anatomy of stone morphology	Microscopic reference images	Endoscopic images
Surface: Large rod-shaped crystals thereafter evolving toward slightly rough or resembling cabbage, whitish or beige surface		
Section: Compact radial crystallisation with locally concentric layers		
Common Aetiology:	*Hypercalciuria: primary hyperparathyroidism, phosphate leak, medullary sponge kidney*	

Conclusion

The present study provided an 81.6% concordance between endoscopic and microscopic urinary stone characterisations. We created didactic boards of confirmed endoscopic images for the most frequently encountered urinary pure stones, including whewellite (Ia or Ib, Id, Ie), weddellite (IIa or IIb), uric acid (IIIa or IIIb), carbapatite (IVa or IVb), brushite (IVd) and cystine (Va or Vb). These boards can be used by urologists to learn how to recognise stones *in situ* using an endoscopic examination before they are destroyed. Thereby, urologists must be more involved in the aetiological diagnosis, as well as in the therapeutic nephrolithiasis strategy, to maintain an essential role in the decision tree of urinary stone management.

This first series of endoscopic images will be supplemented by more stone images in future studies to increase the number of examples of rarer urinary stones. This task is already in progress at our institution and will rely on the epidemiological distribution of the occurrence of urinary stones to obtain a sufficiently large population for an opposable statistical approach.

Accurate ESR of the most frequently encountered urinary stone morphologies allows for the development of an endoscopic stone image database designed for automatic computer-aided *in situ* recognition.

Conflicts of Interest

Jean-Christophe Bernhard reports grants and personal fees from Intuitive Surgical, personal fees from Ipsen, BMS, grants from Pfizer, Stratasys; non-financial support from Fujifilm, outside the submitted work. Olivier Traxer reports personal fees from Coloplast, IPG Medical, Olympus, EMS, ROCAMED, Boston Scientific, during the conduct of the study. Michel Daudon reports personal fees from Advicenne, outside the submitted work. Vincent Estrade reports personal fees from Coloplast, Boston Scientific, outside the submitted work. Christophe Almeras, Gregoire Robert, Paul Meria, Baudouin Denis de Senneville, and Franck Bladou have nothing to disclose.
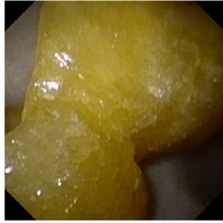
Fig. 9 Pure stone Type Va.

Figure N°9: Pure stone Type Va		
	Pure Stone Type Va: Component <u>cystine</u> N = 7: good match = 100% *P* = NS	
Descriptive anatomy of stone morphology	Microscopic reference images	Endoscopic images
Surface: Homogeneous, bumpy or rough, waxy in colour homogeneous brown-light yellow		
Section: Diffuse or unorganised radial, light brown-yellow		
Common aetiology:	*Cystinuria*	

Table 2 Matched results between endoscopic and microscopic studies.

Stone Type	Good match, n (%)	Bad match, n (%)	Total, n	P	AUC	Sensitivity, %	Specificity, %	PPV, %	NPV, %	FPR, %	FNR, %
Ia or Ib	175 (85)	30 (15)	205	NS	0.87	85	88	89	85	12	15
Ia active	7 (100)	0 (0)	7	/	/	/	/	/	/	/	/
Id	12 (92)	1 (8)	13	NS	0.96	92	99	80	100	1	8
Ie	4 (80)	1 (20)	5	NS	0.90	80	100	100	100	0	20
IIa or IIb	151 (85)	27 (15)	178	NS	0.87	85	88	86	88	12	15
IIIa or IIIb	58 (91)	6 (9)	64	NS	0.95	91	99	94	98	1	9
IIIc	0 (0)	3 (100)	3	/	/	/	/	/	/	/	/
IVa1	142 (81)	34 (19)	176	0.03	0.86	81	91	88	85	9	19
IVa2	3 (21)	11 (79)	14	0.02	0.6	21	99	43	97	1	79
IVb	5 (50)	5 (50)	10	NS	0.74	50	98	45	99	2	50
IVc	9 (75)	3 (25)	12	0.001	0.86	75	96	39	99	4	25
IVd	15 (65)	8 (35)	23	NS	0.82	65	99	83	98	1	35
Va	7 (100)	0 (0)	7	/	/	/	/	/	/	/	/
VIa or VIb	2 (33)	4 (67)	6	NS	0.67	33	100	100	99	0	67
Total	590 (82)	133 (18)	723	–	–	–	–	–	–	–	–

P values denoted by '/' correspond to data that are insufficiently populated for the statistical comparison. Non-significant differences between the endoscopic and microscopic analyses are denoted by 'NS'. AUROC, sensitivity, specificity, PPV, NPV, FPR and FNR are reported only for non-significant differences between the endoscopic and microscopic findings. FNR, false-negative rate; FPR, false predictive rate.

References

1 **Daudon M, Bader CA, Jungers P**. Urinary calculi: review of classification methods and correlations with etiology. *Scanning Microsc* 1993; 7: 1081–104

2 **Daudon M, Jungers P, Bazin D, Williams JC Jr**. Recurrence rates of urinary calculi according to stone composition and morphology. *Urolithiasis* 2018; 46: 459–70

3 **Cloutier J, Villa L, Traxer O, Daudon M**. Kidney stone analysis: "Give me your stone, I will tell you who you are!". *World J Urol* 2015; 33: 157–69

4 **Estrade V, Daudon M, Méria P, Traxer O**. [Why should urologist recognize urinary stone and how? The basis of endoscopic recognition] [Article in French]. *Prog Urol* 2017; 27: F26–35

5 **Daudon M, Dessombz A, Frochot V et al**. Comprehensive morpho-constitutional analysis of urinary stone improves etiological diagnosis and therapeutic strategy of nephrolithiasis. *C R Chim* 2016; 19: 1470–91

6 **Emiliani E, Talso M, Cho SY et al**. Optimal settings for the noncontact Holmium:YAG stone fragmentation popcorn technique. *J Urol* 2017; 198: 702–6

7 **Doizi S, Keller EX, De Coninck V, Traxer O**. Dusting technique for lithotripsy: what does it mean? *Nat Rev Urol* 2018; 15: 653–4

8 **Keller EX, De Coninck V, Doizi S, Daudon M, Traxer O**. Thulium fiber laser: ready to dust all urinary stone composition types? *World J Urol* 2020; 38: 1883–94. https://doi.org/10.1007/s00345-020-03217-9

9 **Doizi S, Raynal G, Traxer O**. [Evolution of the stone treatment over 30 years in a French academic institution] [Article in French]. *Prog Urol* 2015; 25: 543–8

10 **Carpentier X, Meria P, Bensalah K et al**. [Update for the management of kidney stones in 2013. Lithiasis Committee of the French Association of Urology] [Article in French]. *Prog Urol* 2014; 24: 319–26

11 **Chabannes E, Bensalah K, Carpentier X et al**. [Management of adult's renal and ureteral stones. Update of the Lithiasis Committee of the French Association of Urology (CLAFU). General considerations] [Article in French]. *Prog Urol* 2013; 23: 1389–99

12 **Estrade V, Bensalah K, Bringer JP et al**. [Place of the flexible ureterorenoscopy first choice for the treatment of kidney stones. Survey results practice committee of the AFU lithiasis completed in 2011] [Article in French]. *Prog Urol* 2013; 23: 22–8

13 **Raynal G, Merlet B, Traxer O**. [In-hospital stays for urolithiasis: analysis of French national data] [Article in French]. *Prog Urol* 2011; 21: 459–62

14 **Traxer O, Lechevallier E, Saussine C**. [Flexible ureteroscopy with Holmium laser: technical aspects] [Article in French]. *Prog Urol* 2008; 18: 929–37

15 **Traxer O, Lechevallier E, Saussine C**. [Flexible ureteroscopy with Holmium laser: the tools] [Article in French]. *Prog Urol* 2008; 18: 917–28

16 **Bergot C, Robert G, Bernhard JC et al**. [The basis of endoscopic stones recognition, a prospective monocentric study] [Article in French]. *Prog Urol* 2019; 29: 312–7

17 **Black KM, Law H, Aldoukhi A, Deng J, Ghani KR**. Deep learning computer vision algorithm for detecting kidney stone composition. *BJU Int* 2020; 125: 920–4

18 **Daudon M, Traxer O, Lechevallier E, Saussine C**. [Epidemiology of urolithiasis] [Article in French]. *Prog Urol* 2008; 18: 802–14

19 **Andreeva V, Vinarov A, Yaroslavsky I et al**. Preclinical comparison of superpulse thulium fiber laser and a holmium:YAG laser for lithotripsy. *World J Urol* 2020; 38: 497–503

20 **Traxer O, Keller EX**. Thulium fiber laser: the new player for kidney stone treatment? A comparison with Holmium:YAG laser. *World J Urol* 2020; 38: 1883–94

21 **Almeras C, Daudon M, Estrade V, Gautier JR, Traxer O, Meria P**. Classification of the renal papillary abnormalities by flexible ureteroscopy: evaluation of the 2016 version and update. *World J Urol* 2020. https://doi.org/10.1007/s00345-020-03149-4

Correspondence: Vincent Estrade, Department of Urology, CHU Pellegrin, Place Amelie Raba Leon, 33000 Bordeaux, France.

e-mail: vincent.estrade@gmail.com

Abbreviations: AUROC, area under the receiver ROC curve; CCD sensor, Charge-Coupled Device sensor; ESR, endoscopic stone recognition; FTIR, Fourier transform-infrared spectroscopy; LASER, Light Amplification by Stimulated Emission of Radiation; (N)(P)PV, (negative) (positive) predictive value; ROC, receiver operating characteristic.